

Triangular Mesh Construction Based on Point Cloud Matrix and Edge Feature Extraction*

Jinyun Sun and Yong Jiang

College of Automation and Electrical Engineering,
Shenyang Ligong University
the State Key Laboratory of Robotics,
Shenyang Institute of Automation,
Chinese Academy of Sciences
Shenyang, China
sunjinyun@sia.cn, jiangyong@sia.cn

Jing Jiang

College of Automation and Electrical Engineering,
Shenyang Ligong University
Shenyang, China
jiang43@sohu.com

Xiaobao Bai

State Grid Shanxi Electric Power Company Taiyuan, China
cgybx1979@163.com

Abstract—This paper builds a 3D laser scanner by a one-dimensional pitching rotation pan-tilt and a 2D laser range finder to get the 3D laser point cloud data from the motion environment. Depends on this data, a triangular mesh construction algorithm based on the point cloud matrix is proposed to construct the triangular mesh of the motion environment. Then a triangular plane normal vector clustering algorithm is used to extract the edge feature from the triangular mesh and the mean square deviation is employed as further process to make the edge feature more accurately. The experiment results show that the triangular mesh of motion environment can be constructed effectively and edge feature can be exacted accurately by the algorithms applied above. It lays the foundation of mobile robot autonomous movement in unknown complex environments.

Keywords—point cloud data; 2D laser range finder; point cloud matrix; triangular mesh; edge feature extraction

I. INTRODUCTION

3D laser scanning technology is a high-tech technology in the mid ninety's of last century, which is a new method to obtain the 3D coordinates of the object surface by the high-speed laser scanning. This technology is also used in the field of mobile robot widely[1-3]. It is great significance for the mobile robot to identify obstacles in unknown environments. We need to obtain the environmental information as much as possible by using a effective laser sensor.

Triangles have the advantages of flexible structure and good boundary adaptability. It is especially suitable for surface reconstruction of spatial point cloud data. The more commonly used approach is the 3D Delaunay triangulation of the point cloud data, such as α -shape, Voronoi, Crust algorithm and so on. α -shape algorithm is to delete the tetrahedral in the tetrahedral convex hull which the radius of the surround ball or circumcircle is greater than α to get the surface reconstruction[4]. Mrigot et al proposed a theory of "Voronoi covariance". This method based on a covariance matrix of Voronoi diagram to obtain the local main curvature and the main direction of the point cloud surface. The feature points

This work was supported by the Key Program of the Chinese Academy of Sciences (Grant No. KGZD-EW-608-1), the Science and Technology Department of Liaoning Province (Grant No. 2015106014), and the State Key Laboratory of Robotics (Grant No. 2014-Z09).

are extracted by changing the local neighborhood size iterative calculation of covariance matrix[5,6]. Crust algorithm[7-11] is proposed by Amenta et al. The algorithm is based on Voronoi graph and Delaunay triangulation. The advantage of Crust algorithm is that the idea is direct, simple and the reconstruction effect is more precise. It can realize the curve reconstruction of the sampling point set such as with point of density in the detail area or with the sparse point in the area of no characteristic area and less characteristic area. Giaccari Luigi's grid algorithm is a method to remove the redundant triangular facet to extract the triangular facet of the model surface[12]. The algorithm supports reconstruction of irregular surface and can be applied to any types of open surface. The most important is that the algorithm can be applied to the surface with holes.

The above methods are more effective for uniform point cloud data. But because the scanning surface of the point cloud data with nonuniformity or discontinuity, it is hard to build triangular element which is needed sometimes. It even introduce some interference triangular element and seriously influence the effect of mesh construction. In this paper, a triangular mesh construction algorithm based on point cloud matrix is proposed. It can reconstruct the triangular mesh which similar to the topology of original environment. It also effectively avoid cross disorder and interference defects of triangular element in the mesh. Depend on this, the boundary feature extraction is carried out by using the triangular plane normal vector clustering algorithm. It obtains the edge feature information of the motion environment. And the edge feature information lays the foundation for mobile robot autonomous movement in unknown environments. Finally, the validity of the above algorithms are verified by the experimental results of indoor environment.

II. THE 3D LASER SCANNING SYSTEM

The 3D laser scanning system is made up of the 2D laser range finder, one-dimensional pitching rotation pan-tilt and host computer of three parts, as shown in Fig. 1. Where

$\{X_g, Y_g, Z_g\}$ is base coordinate system, $\{X_s, Y_s, Z_s\}$ is coordinate system of laser range finder. Fan-shaped area is the scanning range of 2D laser range finder. The 2D laser range finder and the pitching rotation pan-tilt are mainly used for scanning 3D environment and host computer is mainly used for real-time processing of scanning data.

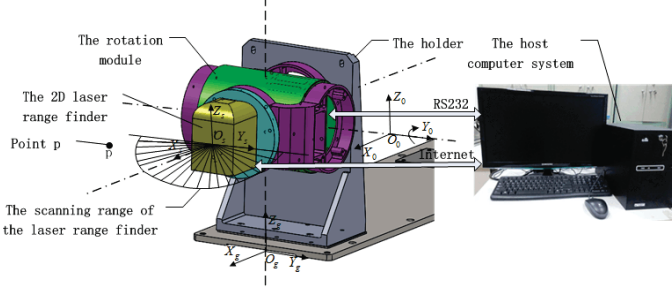


Fig. 1. The 3D laser scanning system

The 2D laser sensor used in this paper is UTM30LX which produced by HOKUYO company. The 2D laser sensor has some characteristics, such as high accuracy, high resolution, wide field of view and so on. It has the advantage of compact structure, light weight and low power consumption. It is ideal for mobile robots to detect environment. The measuring range of UTM30LX is 0.1m to 30m and the measuring accuracy is $\pm 30\text{mm}$. The measuring angle range from 0° to 270° . Angular resolution is 0.25° . The input voltage is DC12V. The scanning frequency is 40Hz which can meet the most demand of acquisition of 3D scene information indoor or outdoor. UTM30LX communicates with the host computer via Ethernet. The one-dimensional pitching rotation pan-tilt is composed by the rotation module and the holder. The rotating shaft of rotating module parallel with the bottom surface of the holder. The rotating module is rotated in the range of -60° ~ 90° and the rate of rotation is $2.5^\circ/\text{s}$. The rotation module communicates with the host computer by CAN bus. The PC software enables real-time monitoring the rotation module.

When the scanning system is working properly, the host computer controls the rotation pan-tilt at a given rotational speed and drives the 2D laser range finder which fixed on the front of the pan-tilt rotates around y axis. The host computer synchronously records the rotation angle of the rotation pan-tilt and the depth information of the environmental produced by the 2D laser range finder.

III. TRIANGULAR MESH CONSTRUCTION

A. Preprocess of point cloud data

The 2D laser range finder and the one-dimensional pitching rotation pan-tilt synchronous sampling is the key to realize 3D laser scanning. It records environment depth information and rotation angle of pan-tilt synchronously. The specific coordinates of the scanning point under the base coordinate can be calculated by coordinate transformation.

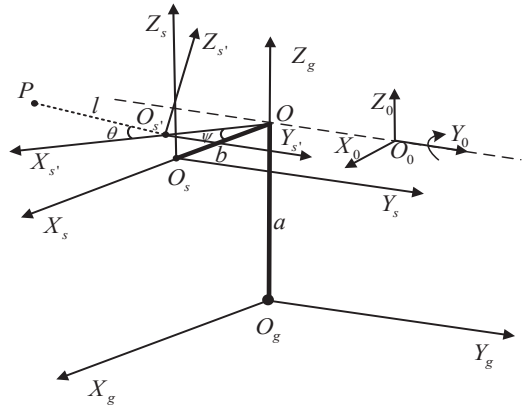


Fig. 2. Point cloud data coordinate system transformation

A 3D scene base coordinate system $\{X_g, Y_g, Z_g\}$ is established based on the ground plane, as shown in Fig.2. $\{X_s, Y_s, Z_s\}$ is the 2D laser range finder coordinate system and the pitch angle is $\psi = 0^\circ$ at this moment. When the pitching rotation pan-tilt rotates ψ around Y_0 the axis, the 2D laser range finder coordinate system becomes $\{X_{s'}, Y_{s'}, Z_{s'}\}$. P is one of ranging point of the laser range finder. θ is the included angle between $PO_{s'}$ and $Y_{s'}$ axis. l is the length of $PO_{s'}$. The coordinate of P in $\{X_{s'}, Y_{s'}, Z_{s'}\}$ is:

$$\begin{bmatrix} X_{s'} \\ Y_{s'} \\ Z_{s'} \end{bmatrix} = \begin{bmatrix} l \cos \theta \\ l \sin \theta \\ 0 \end{bmatrix} \quad (1)$$

The coordinate in the base coordinate system is:

$$\begin{bmatrix} X_g \\ Y_g \\ Z_g \end{bmatrix} = \begin{bmatrix} \cos \psi & 0 & \sin \psi \\ 0 & 1 & 0 \\ -\sin \psi & 0 & \cos \psi \end{bmatrix} \begin{bmatrix} l \cos \theta \\ l \sin \theta \\ 0 \end{bmatrix} + \begin{bmatrix} b \cos \psi \\ 0 \\ a - b \sin \psi \end{bmatrix} \quad (2)$$

Where a is the distance between Y_0 and Y_g . b is the length of $OO_{s'}$. The point O is the intersection of Y_0 and X_s . After calibration, $a = 230\text{mm}$, $b = 130\text{mm}$, $\theta \in [-90^\circ, 90^\circ]$ and $\psi \in [-40^\circ, 40^\circ]$.

B. Point cloud data compression

It should compress the point cloud data appropriately in order to realize the triangular mesh construction of the point cloud matrix more quickly and reduce the time and resources consumed by point cloud over dense. The ultimate goal of the point cloud compression is to reduce the number of point cloud and to retain environment information as much as possible. It does not change the original characteristics of the environment after processing. According to the working principle of the 2D laser range finder and the actual working condition of the mobile robot, the uniform sampling method is used to compress the point cloud data. The method steps are as follows:

1) From the first set of single scan data, every 250ms takes a set of single scan data.

2) The scanning time of the laser range finder is 25ms/scan, and the number of points in a single scan is fixed. According to the scanning order of the measurement points, from the first point of a single scan record a point data every 10 point.

The method is simple and simplifies the point cloud data quickly. There is no need to search for the neighborhood data points, just take points according to the scanning order of the point cloud data, so the processing speed is fast. The method can be relatively complete to retain the overall profile of the environment after compression and facilitate to the subsequent processing of the point cloud data.

C. Construction triangular mesh

Discrete 3D laser spots can not reflect the actual state of the environment and can not conducive describe the surface feature of an actual object. It need to build mesh on the point cloud. Triangle suitable for space point cloud surface reconstruction especially because of flexible structure and better border adaptability. Currently, there is a variety of mature algorithms to use triangular mesh structure a continuous smooth surface. But how to triangulate point cloud on the space surface is always the difficulty of the whole problem.

In this paper, the mesh construction of the laser point cloud is realized by using the triangular elements and a triangular mesh construction algorithm based on point cloud matrix is proposed.

Point cloud matrix P is defined as follows:

$$P = \begin{bmatrix} p_{1,1} & p_{1,2} & \cdots & p_{1,j} & \cdots & p_{1,n} \\ p_{2,1} & p_{2,2} & \cdots & p_{2,j} & \cdots & p_{2,n} \\ \vdots & \vdots & & \vdots & & \vdots \\ p_{i,1} & p_{i,2} & \cdots & p_{i,j} & \cdots & p_{i,n} \\ \vdots & \vdots & & \vdots & & \vdots \\ p_{m,1} & p_{m,2} & \cdots & p_{m,j} & \cdots & p_{m,n} \end{bmatrix} \quad (3)$$

Where, element

$$p_{i,j} = x_{i,j}\mathbf{i} + y_{i,j}\mathbf{j} + z_{i,j}\mathbf{k} \quad (i=1,2,\dots,m; j=1,2,\dots,n)$$

indicates the distance measuring point of the host computer record.

In order to facilitate the division of the triangular mesh, the elements of the point cloud matrix P are set partitioning.

The point cloud set as follows:

$$\mathcal{Q}_t = Q_{(i-1)(n-1)+j} = \{p_{i,j}, p_{i,j+1}, p_{i+1,j}, p_{i+1,j+1}\} \quad (i=1,2,\dots,m-1; j=1,2,\dots,n-1) \quad (4)$$

Then

$$P \Rightarrow Q = \{\mathcal{Q}_1, \mathcal{Q}_2, \mathcal{Q}_3, \dots, \mathcal{Q}_t, \dots, \mathcal{Q}_{(m-1)(n-1)}\} \quad (5)$$

$$(t=1,2,\dots,(m-1)(n-1))$$

The \mathcal{Q}_t is constructed by triangles, respectively:

$$\Delta p_{i,j} p_{i,j+1} p_{i+1,j} \quad (6)$$

$$\Delta p_{i,j+1} p_{i+1,j} p_{i+1,j+1} \quad (7)$$

A total of $2(m-1)(n-1)$ triangles are constructed after traversing all the elements in the set Q . The point cloud matrix P is constructed to triangular mesh.

The algorithm has the following advantages:

- The surface reconstruction of 3D point cloud data supports structured environment. It can be applied to the open surface.
- The principle of the algorithm is simple, easy to implement and running faster.
- It can construct the surface mesh of the non-uniform point cloud matrix model, more complete retention of the original model topology. It preserves the topology of the original model completely.

IV. EXTRACT BOUNDARY FEATURE OF THE POINT CLOUD

It needs to obtain the boundary information of the obstacle environment, in order to make the mobile robot realize obstacle negotiation or obstacle avoidance function in an unknown environment. The boundary information of the point cloud matrix is extracted by using triangle plane normal vector clustering algorithm.

$\Delta p_{i,j} p_{i,j+1} p_{i+1,j}$ and $\Delta p_{i,j+1} p_{i+1,j} p_{i+1,j+1}$, normal vectors of these two triangles are as follows:

$$\mathbf{n}_{f1} = \frac{(p_{i+1,j} - p_{i,j}) \times (p_{i,j+1} - p_{i,j})}{\|(p_{i+1,j} - p_{i,j}) \times (p_{i,j+1} - p_{i,j})\|} \quad (i=1,2,\dots,m-1; j=1,2,\dots,n-1) \quad (8)$$

$$\mathbf{n}_{f2} = \frac{(p_{i+1,j} - p_{i,j+1}) \times (p_{i+1,j+1} - p_{i,j+1})}{\|(p_{i+1,j} - p_{i,j+1}) \times (p_{i+1,j+1} - p_{i,j+1})\|} \quad (i=1,2,\dots,m-1; j=1,2,\dots,n-1) \quad (9)$$

Where $f1 = 2t - 1 = 2[(i-1)(n-1) + j] - 1$,

$$f2 = 2t = 2[(i-1)*(n-1) + j]$$

We analyze the difference degree of the two normal vectors which produced by two adjacent triangular elements in the triangle mesh. It is divided into three kinds of situations:

1) $\Delta p_{i,j} p_{i+1,j-1} p_{i+1,j}$ constructed by \mathcal{Q}_{t-1} and $\Delta p_{i,j} p_{i,j+1} p_{i+1,j}$ constructed by \mathcal{Q}_t . The difference degree between the two normal vectors can be written as:

$$dif(\mathbf{n}'_{f1}, \mathbf{n}'_{f2}) = \cos(\mathbf{n}'_{f1}, \mathbf{n}'_{f2}) = \frac{(\mathbf{n}'_{f1}, \mathbf{n}'_{f2})}{\|\mathbf{n}'_{f1}\| \|\mathbf{n}'_{f2}\|} \quad (10)$$

Where $f1 = 2(t-1) = 2[(i-1)(n-1) + j - 1]$,

$$f2 = 2t - 1 = 2[(i-1)(n-1) + j] - 1$$

$$(i=1, 2 \dots, m-1; j=1, 2 \dots, n-1).$$

2) Two normal vectors in the operation are produced by $\Delta p_{i,j} p_{i,j+1} p_{i+1,j}$ and $\Delta p_{i,j+1} p_{i+1,j} p_{i+1,j+1}$, which are constructed by the Q_t . In this case, the difference degree of these normal vectors can be written as:

$$dif(\mathbf{n}_{f1}, \mathbf{n}_{f2}) = \cos(\mathbf{n}_{f1}, \mathbf{n}_{f2}) = \frac{(\mathbf{n}_{f1}, \mathbf{n}_{f2})}{\|\mathbf{n}_{f1}\| \|\mathbf{n}_{f2}\|} \quad (11)$$

Where $f1 = 2t = 2[(i-1)(n-1) + j]$,

$$f2 = 2t - 1 = 2[(i-1)(n-1) + j] - 1$$

$$(i=1, 2 \dots, m-1; j=1, 2 \dots, n-1)$$

3) $\Delta p_{i-1,j+1} p_{i,j} p_{i,j+1}$ constructed by $Q_{i-(n-1)}$ and $\Delta p_{i,j} p_{i,j+1} p_{i+1,j}$ constructed by Q_t . The difference degree between the two normal vectors can be written as:

$$dif(\mathbf{n}''_{f1}, \mathbf{n}''_{f2}) = \cos(\mathbf{n}''_{f1}, \mathbf{n}''_{f2}) = \frac{(\mathbf{n}''_{f1}, \mathbf{n}''_{f2})}{\|\mathbf{n}''_{f1}\| \|\mathbf{n}''_{f2}\|} \quad (12)$$

Where

$$f2 = 2[t - (n-1)] - 1 = 2[(i-1)(n-1) + j - (n-1)] - 1,$$

$$f2 = 2t = 2[(i-1)(n-1) + j]$$

$$(i=1, 2 \dots, m-1; j=1, 2 \dots, n-1)$$

The difference degree range is $[-1, 1]$. To determine whether the two adjacent triangular planes belong to the same plane, we set a threshold value λ . If $\lambda \in (0, 1]$, then the public edge of the two triangular planes may belong to a part of the geometric edge of the environment. If $dif \in (-1, 0]$, then the two triangular planes must not belong to the same plane. If $dif = -1$, the two triangular planes belong to the same plane. But it does not meet the actual situation because of two normal vector difference of 180 degrees, so we set it does not belong to the same plane. If the difference degree is greater than the threshold value λ , it is considered that the two triangular planes in the same plane.

We use the above method to extract the common edges of different triangular planes, these edges are likely to be the boundary of the point cloud data. But the boundary feature information is relatively rough, and it needs to be a further extraction.

Because of the point cloud data nonuniform or the scanning surface discontinuous, the triangular mesh can be constructed with some interference triangle elements. The edges of these triangles are considered to be a part of the geometric edge of the environment mistakenly. In this paper, we extract edge feature accurately by distinguishing the mean square deviation of the public edge length of the triangles.

V. EXPERIMENTAL TESTING AND ANALYSIS

In order to verify the feasibility and effectiveness of the algorithm, experiment is carried out upon the 3D laser scanning system.

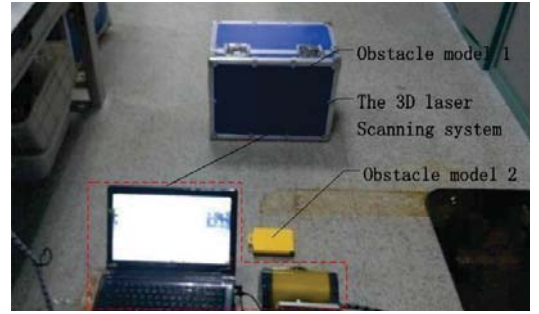


Fig. 3. Experimental environment

Fig.3 is a point cloud data acquisition experimental environment in laboratory. The blue box is the obstacle model 1, the yellow box is the obstacle model 2, the left is the bench and the right lockers. The rotation pan-tilt of the 3D laser scanning system rotates from the bottom up and drives the 2D laser range finder to scan the environment ahead. The host computer records the depth information of environment generated by the laser and records the pitching rotation angle of the rotation pan-tilt synchronously.

We simplify the 3D point cloud model by the point cloud data compression algorithm. Fig.4 is the original 3D laser point cloud image, Fig.5 is the image of the point cloud after using the compression algorithm to deal with the 3D point cloud. It can be seen that the intensive degree of point cloud data has been greatly reduced and the basic shape of the obstacle has been preserved.

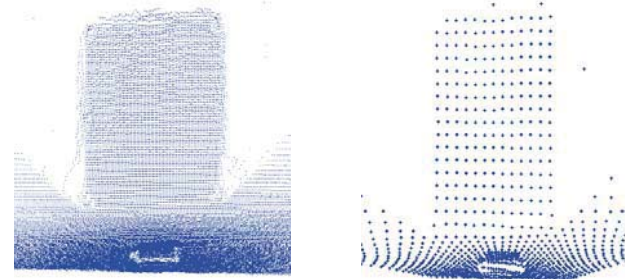


Fig. 4. Obstacles environment point cloud

Figure 5 shows the compressed point cloud. The compressed point cloud retains the basic shape of the obstacles while significantly reducing the density of points, making it more efficient for storage and processing.

Fig. 5. Compressed point cloud

data after compression, (b) is the environment model constructed by Giaccari Luigi mesh construction algorithm, (c) is the triangular mesh constructed by triangular mesh construction algorithm based on point cloud matrix. (d) is the mesh of obstacles.

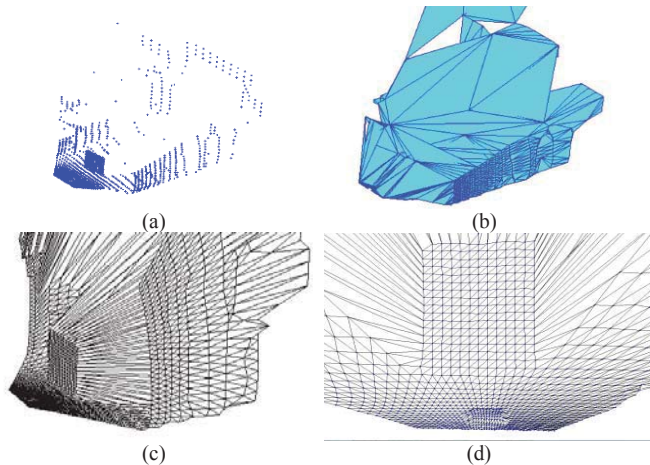


Fig. 6. Triangular mesh construction

Experiments show that because of the nonuniform and the discontinuity of the scanning surface of the point cloud data, the Giaccari Luigi mesh construction algorithm is not ideal. It can not be a good reduction of the current motion environment, and introduction a lot of inferential triangular elements. The triangular mesh construction based on the point cloud matrix constructs the triangular mesh more clearly. It is not affected by the nonuniform and the discontinuity of the scanning surface of the point cloud data. It reduces the current situation of the motion environment preferably and preserves the boundaries of the obstacle information.

The boundary feature information of point cloud data is extracted by using triangular plane normal vector clustering algorithm. The experimental results are shown in Fig.8.

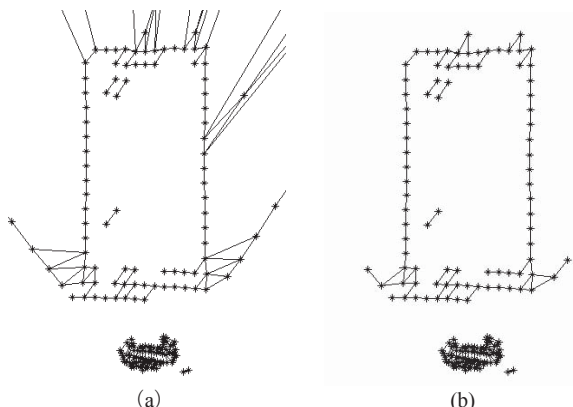


Fig. 7. The boundary feature of point cloud extraction

(a) is the obstacle boundary feature extracted by triangular plane normal vector clustering algorithm. (b) is the obstacle boundary feature extracted by the mean square deviation. It is known from the comparison that the triangular plane normal

vector clustering algorithm can preliminary extract the boundary features of the point cloud. The more accurate obstacle boundary information can be obtained by the method of mean square deviation.

CONCLUSIONS

This article takes 3D laser point cloud data as the research object. Depends on this data, a triangular mesh construction algorithm based on the point cloud matrix is proposed to construct the triangular mesh of the motion environment. Then a triangular plane normal vector clustering algorithm is used to extract the edge feature from the triangular mesh and the mean square deviation is employed as further process to make the edge feature more accurately. The experiment results show that the triangular mesh of motion environment can be constructed effectively and edge feature can be exacted accurately by the algorithms applied above. It lays the foundation of mobile robot autonomous movement in unknown complex environments.

REFERENCES

- [1] S. Árni Guðmundsson, M. Pardàs, J. R. Casas, J. R. Steinsson, H. Aanæs, and R. Larsen, "Improved 3D reconstruction in smart-room environments using ToF imaging," *Computer Vision and Image Understanding*, vol. 114, 12// 2010, pp. 1376-1384.
- [2] XIN Yu, LIANG Huawei, MEI Tao, et al., "Dynamic Obstacle Detection and Representation Approach for Unmanned Vehicles Based on Laser Sensor," *ROBOT*, vol. 36, 2014, pp. 654-661.
- [3] WANG Jiaolong, ZHOU Jie, GAO Hui, et al., "Obstacle Avoidance Method for Mobile Robots Based on the Identification of Local Environment Shape Features," *Information and Control*, vol. 44, 2015, pp. 91-98.
- [4] H. Edelsbrunner, E. P. M. #252, and cke, "Three-dimensional alpha shapes," *ACM Trans. Graph.*, vol. 13, 1994, pp. 43-72.
- [5] Q. M. #233, rigot, M. Ovsjanikov, and L. Guibas, "Robust Voronoi-based curvature and feature estimation," presented at the 2009 SIAM/ACM Joint Conference on Geometric and Physical Modeling, San Francisco, California, 2009.
- [6] Me, x, Q. rigot, M. Ovsjanikov, and L. Guibas, "Voronoi-Based Curvature and Feature Estimation from Point Clouds," *Visualization and Computer Graphics, IEEE Transactions on*, vol. 17, 2011, pp. 743-756.
- [7] N. Amenta, M. Bern, and M. Kamvysselis, "A new Voronoi-based surface reconstruction algorithm," presented at the Proceedings of the 25th annual conference on Computer graphics and interactive techniques, 1998.
- [8] N. Amenta and M. Bern, "Surface Reconstruction by Voronoi Filtering," *Discrete & Computational Geometry*, vol. 22, 1999/12/01 1999, pp. 481-504.
- [9] D. Cohen-Steiner and F. Da, "A greedy Delaunay-based surface reconstruction algorithm," *The Visual Computer*, vol. 20, 2004/04/01 2004, pp. 4-16.
- [10] T. K. Dey and S. Goswami, "Provable surface reconstruction from noisy samples," presented at the Proceedings of the twentieth annual symposium on Computational geometry, Brooklyn, New York, USA, 2004.
- [11] M. Ji, F. Hsi-Yung, and W. Lihui, "Delaunay-based triangular surface reconstruction from points via Umbrella Facet Matching," in *Automation Science and Engineering (CASE), 2010 IEEE Conference on*, 2010, pp. 580-585.
- [12] Giaccari L. Surface Reconstruction from Scattered Points Cloud: MyCrust Robust. [2010-3-5]. <http://www.Advancedmcodes.org/surface-reconstruction-from-scattered-points-cloud-mycrust-robust.html>.